Friction and Wear Properties of Polyimide Matrix Composites Reinforced with Short Basalt Fibers

Xinrui Zhang,[1,2] Xianqiang Pei,[1] Qihua Wang[1]

[1]*State Key Laboratory of Solid Lubrication, Lanzhou Institute of Chemical Physics, Chinese Academy of Sciences, Lanzhou 730000, China*
[2]*Graduate School, Chinese Academy of Sciences, Beijing 100039, China*

Received 31 March 2008; accepted 18 September 2008
DOI 10.1002/app.29353
Published online 5 December 2008 in Wiley InterScience (www.interscience.wiley.com).

ABSTRACT: Short basalt fiber (BF) reinforced polyimide (PI) composites were fabricated by means of compression-molding technique. The friction and wear properties of the resulting composites sliding against GCr15 steel were investigated on a model ring-on-block test rig under dry sliding conditions. The morphologies of the worn surfaces and the transfer films that formed on the counterpart steel rings were analyzed by means of scanning electron microscopy. The influence of the short BF content, load, and sliding speed on the tribological behavior of the PI composites was examined. Experimental results revealed that the low incorporation of BFs could improve the tribological behavior of the PI composites remarkably. The friction coefficient and wear rate decreased with increases in the sliding speed and load, respectively. The transfer film that formed on the counterpart surface during the friction process made contributions to reducing the friction coefficient and wear rate of the BF-reinforced PI composites. © 2008 Wiley Periodicals, Inc. J Appl Polym Sci 111: 2980–2985, 2009

Key words: composites; fibers; polyimides

INTRODUCTION

Polymer-based materials have been preferred in recent years over metal-based counterparts because of their low coefficients of friction and ability to sustain loads. In particular, polymer matrix composites reinforced with fibers have been widely accepted as tribo-materials and are used in components supposed to run without any external lubricants.[1,2] Many researchers have made lots of attempts to understand the modifications of the tribological behavior of polymers by the addition of fillers or fiber reinforcements.[3,4] The tribological behavior of polymers exhibits a strong dependence on the imposed friction conditions, such as the sliding velocity and applied load.[5–12] Generally, the formation of a homogeneous transfer film on the counterpart surface improves the tribological performance by reducing the direct contact between the sliding pairs. Many investigations have shown that the incorporation of fiber reinforcements improves the wear resistance and reduces the coefficient of friction. This is attributed to a reduction in ploughing, tearing, and other nonadhesive components of wear by the fibers.[13–18]

Short-fiber-reinforced polymers find applications in various fields of engineering and form a very important class of tribo-materials.[13–18] Despite lower mechanical properties in comparison with continuous fiber-reinforced polymers, short-fiber-reinforced thermoplastics are very attractive because of their easy fabrication, economy, and better mechanical properties in comparison with neat polymers.[14,16] Basalt fibers (BFs), which have better mechanical properties than E-glass fibers and are more widely available and cheaper than carbon fibers, serve as reinforcement materials for a wide range of heat-insulating, filtering, and other materials; they have several advantages, such as the absence of a carcinogenic effect, environmental cleanness, flexibility, good temperature resistance, and heating insulation property, in comparison with glass and asbestos fibers.[19] Polyimide (PI) possesses some extraordinary characteristics, such as excellent mechanical and electrical (insulating) properties, good thermal stability and chemical inertness, high wear resistance, and resistance against high-energy radiation.[20,21] Yet, it cannot be widely used as a self-lubricating material because of its high friction coefficient. Through the

Correspondence to: Q. Wang (wangqh@lzb.ac.cn).
Contract grant sponsor: Innovative Group Foundation of the National Natural Science Foundation of China; contract grant number: 50421502.
Contract grant sponsor: National Natural Science Foundation of China; contract grant number: 50475128.
Contract grant sponsor: Important Direction Project for Knowledge Innovative Engineering of the Chinese Academy of Sciences; contract grant number: KGCX3-SYW-205).

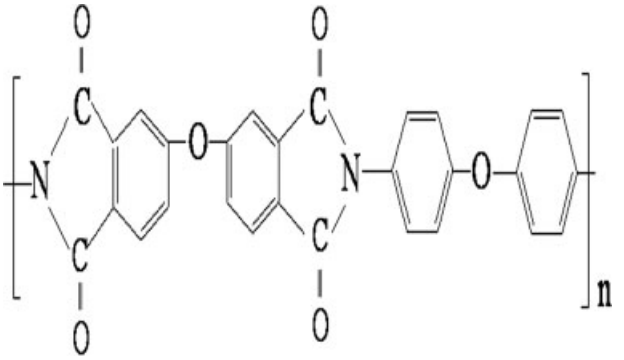

Figure 1 Chemical structure of the PI powder.

reinforcement of PI with BFs, it might be feasible to develop high-performance PI-based composites.

Investigations of BF-reinforced polymer composites have been actively pursued. Currently, most studies have focused on the processes and mechanical and physical properties of BFs. Wang et al.[22] studied the low-velocity impact properties of three-dimensional woven basalt/aramid hybrid composites. The results showed that the interply hybrid composite had higher ductility, a lower peak load, and higher specific energy absorption in both the warp and weft directions versus those of the intraply hybrid composite. Qi et al.[23] fabricated continuous basalt fiber tabby cloth (CBFTC) reinforced S-157 phenolic resin composites and investigated the effects of the resin content on both the mechanical properties and ablative properties of S-157/CBFTC composites. The results showed that the S-157/CBFTC composite with optimal mechanical properties and ablative properties was obtained when the resin content was 30%. However, only a few works have studied the tribological properties of BF-reinforced polymer composites systematically, especially under the condition of a high sliding speed and a heavy load.

BFs can be classified as chopped fibers, continuous fibers, rovings, and fabrics. In this work, PI composites filled with chopped BFs were fabricated. The effects of the short BF content, load, and sliding speed on the tribological properties of the composites were examined in detail. It is expected that this work will lead to new applications of BF-reinforced polymer composites in dry-sliding bearings.

EXPERIMENTAL

Sample preparation

PI (YS-20) powders (<75 μm) were commercially obtained from the Shanghai Synthetic Resin Institute (Shanghai, China). The chemical structure of PI is shown in Figure 1. The short BFs (3–4 mm) were about 13 μm in diameter, and the density was about 2.65 g/cm^3. The commercial short BFs were dipped in acetone for 24 h and then cleaned ultrasonically with acetone for 0.5 h. Finally, they were dried before use. To prepare the PI composite blocks, the mixtures were compressed and heated to 380°C in a mold with intermittent deflation. The pressure was held at 40 MPa for 70 min to allow full compression sintering. At the end of each run of compression sintering, the resulting specimens were cooled with the stove in air and cut into preset sizes for friction and wear tests.

Tribological property testing

The friction and wear behavior of the PI composites sliding against stainless steel rings was evaluated on an M-2000 model ring-on-block test rig (made by the Jinan Testing Machine Factory, Jinan, China), on which friction tests could be performed at low (0.431 m/s) and high speeds (0.862 m/s).The contact schematic diagram is shown in Figure 2; blocks with a size of 30 mm × 7 mm × 6 mm were made of the PI composites, whereas the counterparts were rings of GCr15 stainless steel with a diameter of 40 mm. The chemical composition of the GCr15 bearing steel [mass fraction (%)] is shown in Table I. The tests were carried out at a linear velocity of 0.431 or 0.862 m/s in a period of 120 min with the loads ranging from 200 to 500 N. Before each test, the stainless steel ring and the PI composite block were polished to an average roughness of about 0.2 μm. During the friction process, the block specimen was static, and the steel ring was sliding against the block unidirectionally. The friction force was measured with a torque shaft equipped with strain gauges mounted on a vertical arm that carried the block, which was used to calculate the friction coefficient by taking into account the normal load applied. The wear rate is defined as

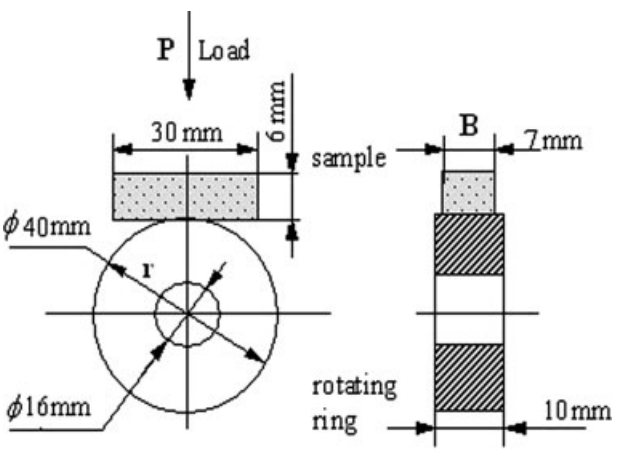

Figure 2 Contact schematic for the friction couple.

TABLE I
Chemical Composition of the GCr15 Steel Ring

Chemical composition (mass fraction, %)					
C	Mn	Si	P	S	Cr
0.95–1.05	0.25–0.45	0.15–0.35	≤0.025	≤0.025	1.40–1.65

the worn volume per unit of load and sliding distance; the inverse of the wear rate is the wear resistance. The width of the wear tracks was measured with a reading microscope to an accuracy of 0.01 mm. Then, the specific wear rate [ω (mm^3/N m)] of the specimen was calculated as follows:

$$\omega = \frac{B}{L^* P}\left[\frac{\pi r^2}{180}\arcsin\left(\frac{b}{2r}\right) - \frac{b}{2r}\sqrt{r^2 - \frac{b^2}{2}}\right] \quad (1)$$

where B is the width of the specimen (mm), r is the semidiameter of the stainless steel ring (mm), b is the width of the wear trace (mm), L is the sliding distance (m), and P is the load (N). The tests were repeated three times, and the average values of the measured friction coefficient and wear rate were used for further analysis. The wear tracks of the composite and stainless steel specimens were examined on a JSM 5600LV scanning electron microscope (JEOL Ltd., Tokyo, Japan). To increase the resolution for the scanning electron microscopy (SEM) observation, the tested composite specimens were plated with a gold coating to render them electrically conductive.

RESULTS AND DISCUSSION

Mass fraction of BFs

The friction coefficient and wear rate of BF/PI composites with various BF contents at a sliding speed of 0.431 m/s under 200 N are shown in Figure 3. The friction coefficient of the pure PI composite was quite high. However, the situation changed greatly when BFs were incorporated. There was a significant reduction in the values of the friction coefficient at a BF content as low as 5 wt %. When the BF contents continued increasing, the declining trend became gentle. In the tested system, with respect to the friction coefficient, the optimum content of BFs was about 10 wt %. The friction coefficient increased with increasing BF content. As for the wear rate, it decreased with an increase in the BF mass content up to 20%, after which it increased. With a high BF content, more PI debris and broken BF fragments appeared on the worn surface (this was supported by SEM, as discussed in the next section) because of the dropout of BFs from the PI matrix during the friction process, which shifted the wear mechanisms from adhesive wear to abrasive wear; this reduced the wear resistance drastically and increased the friction coefficient. For the best combination of the friction coefficient and wear rate, the optimal content of BFs in the PI composite appeared to be 10 wt %. This proportion was chosen to investigate the effects of the sliding speed and load on the friction and wear behavior of the BF/PI composites.

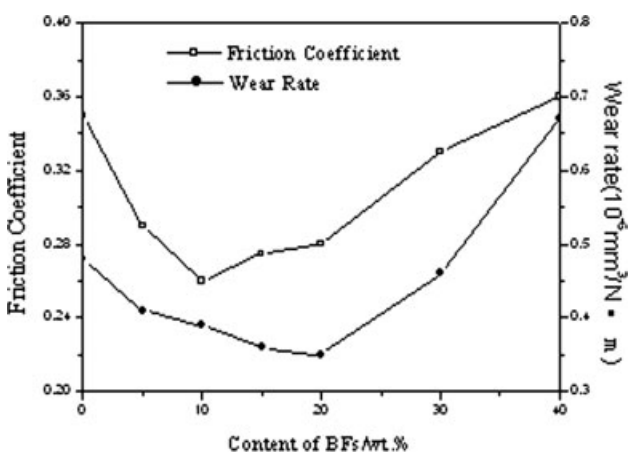

Figure 3 Variations of the friction coefficient and wear rate with the BF content in the BF/PI composites.

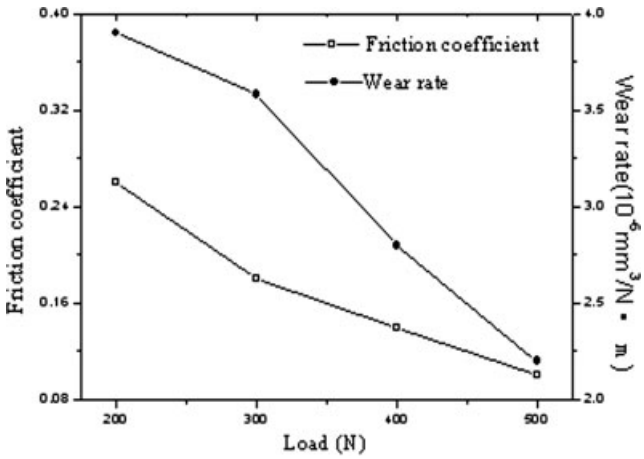

Figure 4 Variations of the friction coefficient and wear rate of the BF/PI composites under different loads.

Load and sliding speed

Variations of the friction and wear properties of the BF/PI composites with the load are shown in Figure 4. The tribological characteristics of the BF/PI composites were very sensitive to the variation of the load. Both the friction coefficient and the wear rate of the BF/PI composites decreased remarkably with an increase in the load. When the applied load was increased, some big particle-shaped or flaky debris on the wear surface was crushed or sheared into

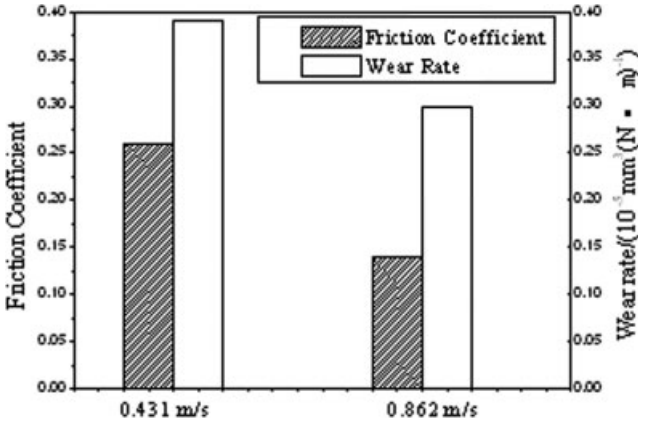

Figure 5 Effect of the sliding speed on the friction and wear of the BF/PI composites.

smaller particles or thinner flakes and acted as a lubricant. Moreover, the transfer film could more easily form because of the increase in the adhesive force between the film and counterpart. Concomitantly with the newly formed debris, a more integrated but thinner film formed on the worn surface. As a result, the smaller debris and more integrated but thinner film on the worn surface brought about smaller coefficients of friction because of the decreased degree of two-body abrasive wear.[24]

Figure 5 presents the friction and wear properties of the BF/PI composites at a low speed (0.431 m/s) and a high speed (0.862 m/s). Both the friction coefficient and wear rate decreased obviously at the high sliding speed in comparison with the low sliding speed. For most polymers, van der Waals and hydrogen bonds are typical factors for the junctions occurring between the two counterparts. The formation and rupture of these junctions control the adhesion component of friction.[25] With an increase in the sliding speed, there is not enough time to produce more adhesive points because of the decreased surface contact time. As a result, the friction force component from adhesion can be greatly reduced, and the transfer film can easily form and is difficult to rupture. Moreover, the reduction of the friction coefficient and wear rate also contributes to the surface softening arising from frictional heating. It is assumed that, under a small load, the interfacial temperature is a crucial factor determining the tribological characteristics.[26] It is commonly believed that heat generation at friction results from the deformation of the material at the actual contact spots. Some processes with their molecular mechanisms are related to the transformation of mechanical energy into heat.[27] Because of the low thermal conductivity of PI, friction-induced heat surely provokes an increase in the contact temperature; an increase in the sliding velocity will result in a higher contact temperature. Because of the effect of thermal softening caused by friction-induced heat, the friction coefficient decreased remarkably.

SEM analysis of the worn surface and counterpart surface

Figures 6 and 7 show SEM analyses of the worn surfaces and transfer films of PI composites sliding against GCr15 steel at a sliding speed of 0.431 m/s under 200 N. The sliding direction of the counterpart is marked with the white arrowhead. The worn surface of the pure PI was characterized by severe plastic deformation and microcracking [Fig. 6(a)],

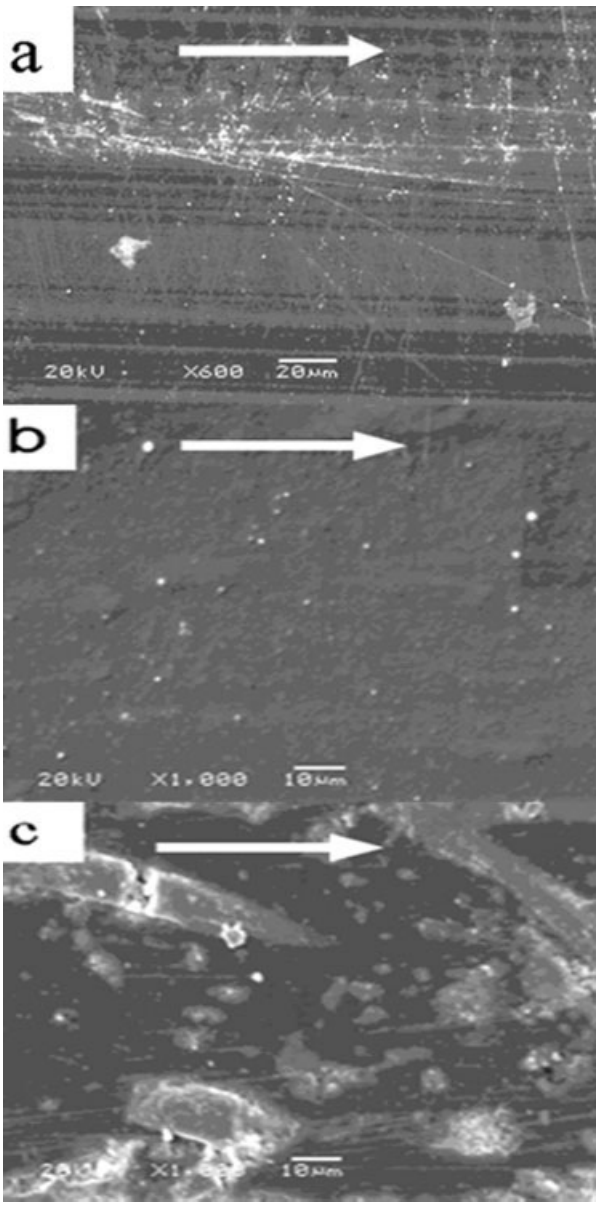

Figure 6 SEM micrographs of the worn surfaces of BF/PI composites: (a) pure PI, (b) 10% BF/PI, and (c) 30% BF/PI.

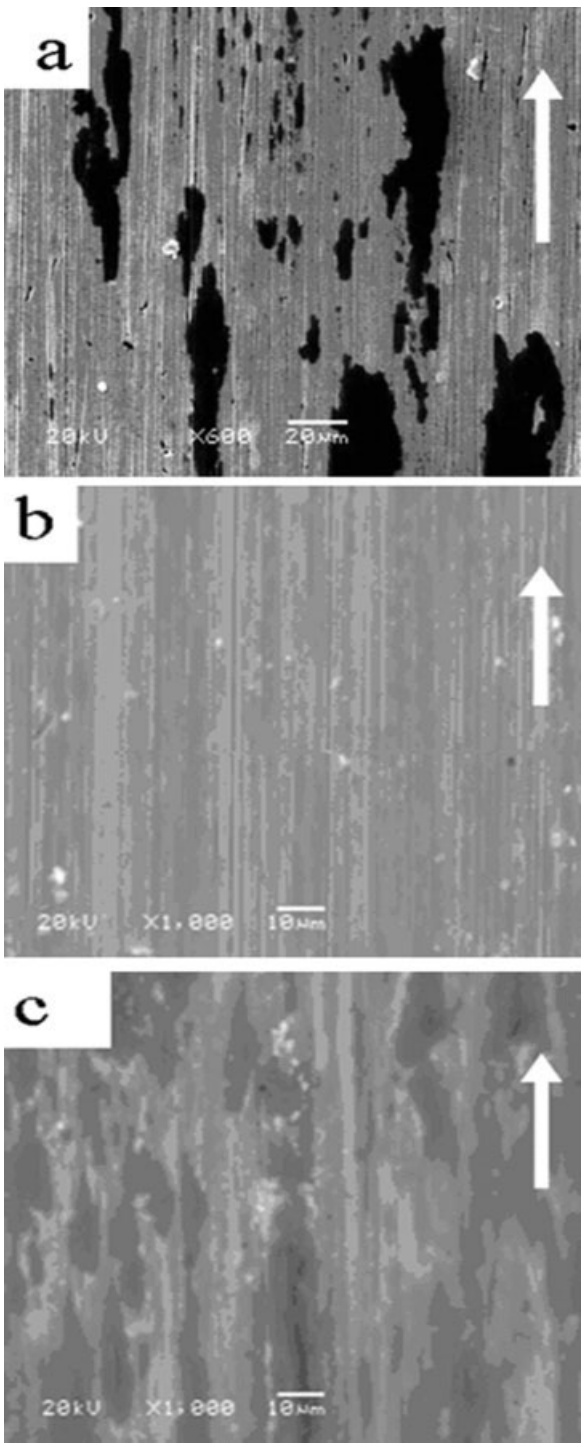

Figure 7 SEM micrographs of the transfer films on the surface of the GCr15 steel counterpart: (a) pure PI, (b) 10% BF/PI, and (c) 30% BF/PI.

whereas a large amount of transferred PI debris was observed on the stainless steel counterpart surface, and the transfer film was thick and discontinuous [Fig. 7(a)]; this corresponded to the high friction coefficient of the pure PI. As for the 10 wt % BF/PI composite, the scuffing and spalling phenomena on the worn surface were significantly abated, there was no obvious plastic deformation [Fig. 6(b)], and the transfer film became comparatively thin and uniform [Fig. 7(b)]. However, the worn surface of the PI composite with 30 wt % BFs [Fig. 6(c)] was characterized by many pullouts and exposures of BFs, and there were more wear debris and BF fragments, which indicated the poor adhesion between the BFs and PI matrix. The dropout of the BFs from the PI matrix shifted the wear mechanisms from adhesive wear to abrasive wear. Meanwhile, the transfer film [Fig. 7(c)] appeared to be thick, rough, and discontinuous on the GCr15 steel counterpart surface.

The worn surface and transfer film generated at 200 N and 0.862 m/s in 120 min are presented in Figure 8. With an increase in the sliding speed, the interfacial bonding between the composite and the counterpart decreased. Moreover, the surface softened because of the increased frictional heat resulting from the deformation of the composite in the actual contact spots. The worn surface became smoother [Fig. 8(a)], and the transfer film [Fig. 8(b)] could easily form, was difficult to rupture, and

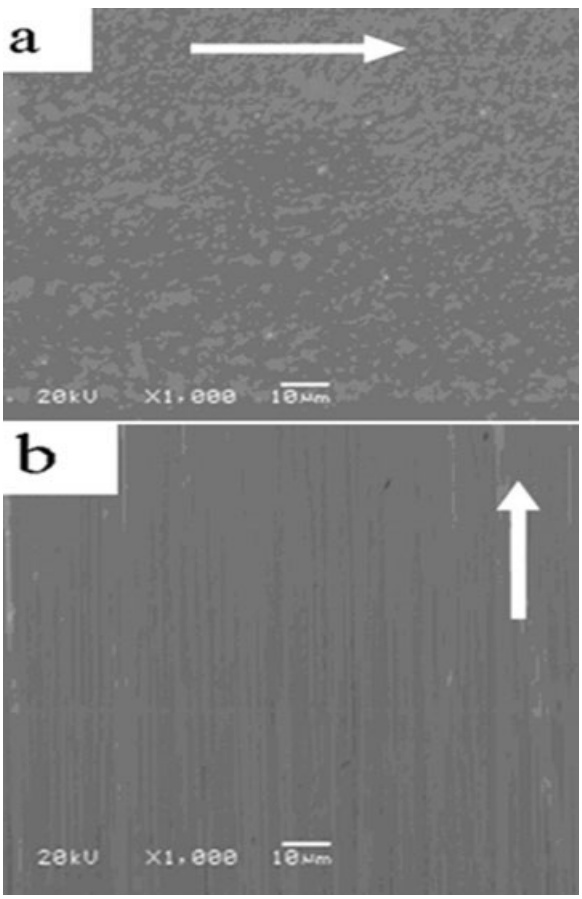

Figure 8 SEM micrographs of (a) the worn surfaces of BF/PI and (b) the transfer films formed on the counterpart steel rings at 200 N and 0.862 m/s.

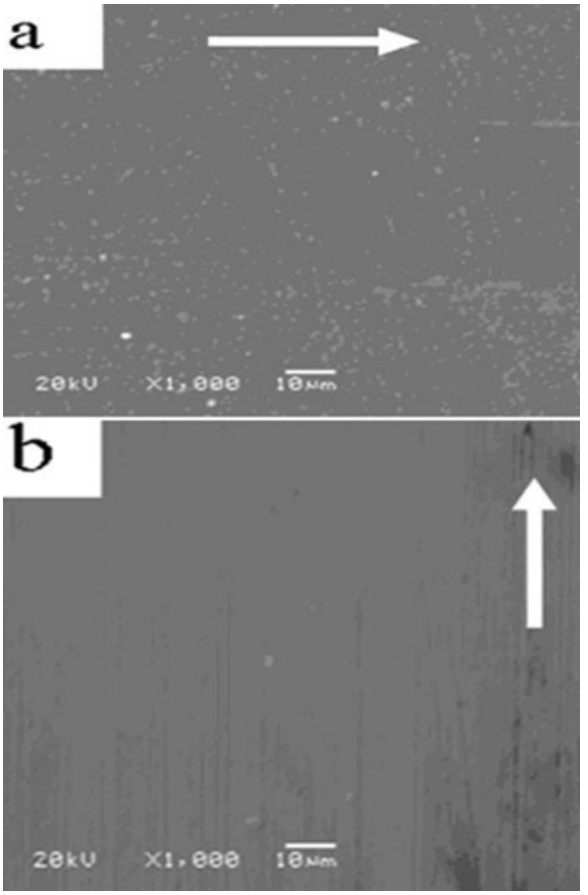

Figure 9 SEM micrographs of (a) the worn surfaces of BF/PI and (b) the transfer films formed on the GCr15 steel rings at 500 N and 0.431 m/s.

became thinner and uniform. With the increase in the load, the transfer film could more easily form because of the increase in the adhesive force between the film and counterpart, and this resulted in a new counter surface producing primarily an adhesive wear mechanism. This mechanism is generally less dangerous for a polymer composite sliding surface than an abrasive one, resulting in a lower friction coefficient and wear rate. The worn surface of the BF/PI composites [Fig. 9(a)] was smoothest, and the transfer film [Fig. 9(b)] was thinnest and continuous. With the formation of a relatively uniform and coherent transfer film, subsequent sliding occurred between the surface of the BF/PI composites and the transfer film. Consequently, a lower friction coefficient and a lower wear rate were reached.

CONCLUSIONS

A systematic investigation of the tribological properties of BF/PI composites was carried out in this work. The following conclusions can be made:

1. An appropriate amount of BFs can improve the tribological properties of PI greatly. For the best combination of the friction coefficient and wear rate, the optimal mass content of BFs in the composites appears to be 10%.
2. The differences in the friction coefficient and wear properties of BF/PI composites are closely related to the sliding conditions, such as the sliding rate and the applied load. Research results show that BF/PI composites exhibited better tribological properties with a higher load and sliding speed.

References

1. Biswas, S. K.; Kalyani, V. Wear 1992, 158, 193.
2. Wang, Y. Q.; Li, J. Mater Sci Eng A 1999, 266, 155.
3. Bijwe, J.; Logani, C. M.; Tewari, U. S. Wear 1990, 138, 77.
4. Wang, J. X.; Gu, M. Y.; Songhao, B.; Ge, S. R. Wear 2003, 255, 774.
5. Lu, Z. P.; Friedrich, K. Wear 1995, 181, 624.
6. Bassani, R.; Levita, G.; Meozzi, M.; Palla, G. Wear 2001, 247, 125.
7. Myshkin, N. K.; Petrokovets, M. I.; Kovalev, A. V. Tribol Int 2005, 38, 910.
8. Bartenev, G. M. Friction and Wear of Polymers; Elsevier: Amsterdam, 1981.
9. Rees, B. L. Research 1957, 10, 331.
10. Flom, D. G.; Porile, N. T. Nature 1955, 175, 682.
11. Flom, D. G.; Porile, N. T. J Appl Phys 1955, 26, 1080.
12. Milz, W. C.; Sargent, L. E. Lubr Eng 1955, 11, 313.
13. Yoo, J. H.; Ess, N. S. Wear 1993, 162, 41.
14. Bijwe, J.; Indumathi, J.; Rajesh, J. J.; Fahim, M. Wear 2001, 249, 715.
15. Xian, G.; Zhang, Z. Wear 2005, 258, 776.
16. Palabiyik, M.; Bahadur, S. Wear 2002, 253, 369.
17. Friedrich, K.; Lu, Z.; Hager, A. M.; Wear 1995, 190, 139.
18. Bahadur, S.; Fu, Q.; Dong, D. Wear 1994, 178, 123.
19. Kuryaeva, R. G.; Kirkinskii, V. A. Phys Chem Miner 1997, 25, 48.
20. Bahadur, S.; Polineni, V. K. Wear 1996, 200, 95.
21. Price, D. M. Thermochim Acta 2001, 367, 253.
22. Wang, X.; Hu, B.; Feng, Y.; Liang, F.; Mo, J. Compos Sci Technol 2008, 68, 444.
23. Qi, F. J.; Li, J. W.; Li, C. X.; Wei, H. Z. Eng Plast Appl 2006, 34, 18.
24. Friedrich, K.; Flock, J.; Varadi, K.; Neder, Z. Wear 2001, 251, 1202.
25. Buckley, D. H. Surface Effects in Adhesion, Friction, Wear, and Lubrication; Elsevier: Amsterdam, 1981.
26. Zhang, G.; Zhang, C.; Nardin, P. Tribol Int 2008, 41, 79.
27. Myshkin, N. K.; Petrokovets, M. I.; Kovalev, A. V. Tribol Int 2005, 38, 910.